2023 14th International Conference on Information and Communication Technology Convergence (ICTC) | 979-8-3503-1327-7/23/$31.00 ©2023 IEEE | DOI: 10.1109/ICTC58733.2023.10392767

Downlink Satellite Network Analysis with Beam Gain in Shadowing Channel

Sungyu Kim, Seunghyeong Yoo*, and Jinseok Choi†
Department of Radio and Information Communications Engineering, Chungnam National University, Republic of Korea
*Department of Electrical Engineering, Ulsan National Institute of Science and Technology, Republic of Korea
†School of Electrical Engineering, Korea Advanced Institute of Science and Technology, Republic of Korea
E-mail: tjsrb724@gmail.com, seunghy@unist.ac.kr, jinseok@kaist.ac.kr

***Abstract*—Satellite communications offer the potential of ensuring global coverage with a substantial capacity. In this paper, we examine the coverage performance of satellite networks by considering a distance-dependent line-of-sight (LOS) and non-LOS (NLOS) channel propagation probability, which takes into account the shadowing effect. Building upon the stochastic geometry-based network analysis used for terrestrial networks, we employ a Poisson point process to model both the satellite network and its users. Through this approach, we derive a theoretical expression for the coverage probability with beam gain under a nearest satellite association rule, providing an analytical understanding of the satellite network. The accuracy of the derived expression is confirmed through simulation results. The derived expression encompasses various network parameters such as satellite density, altitude, channel fading, pathloss, LOS probability, and beam gain, offering valuable insights into satellite networks.**

***Index Terms*—Satellite networks, stochastic geometry, coverage probability, LOS and NLOS channel propagation.**

I. Introduction

The integration of satellite networks with terrestrial cellular networks has garnered significant attention [1], [2]. In particular, low Earth orbit (LEO) satellite networks have emerged as a promising solution for achieving universal coverage with improved data rates and reduced delays compared to traditional geosynchronous equatorial orbit (GEO) satellite networks [3], [4]. To guide the deployment strategy of LEO satellites, it is crucial to understand the coverage and rate performance. In this regard, we employ stochastic geometry techniques to analyze the coverage of satellite downlink networks, taking into account random channel propagation conditions.

In satellite networks, a key distinction from conventional cellular networks when using tools of stochastic geometry is the shape of the network model, which forms a spherical cap within a finite space. This arises from the geometric characteristics of user locations and satellite orbits. In previous studies [3], it was assumed that the distribution of satellite locations follows a homogeneous binomial point process (BPP) on the spherical cap. Moreover, in [5] an analytical expression for coverage was derived specifically for scenarios where satellites function as relays.

While BPPs are valuable for representing evenly distributed satellite placements on a spherical cap, their application in modeling satellite networks is constrained by the assumption that a fixed number of satellites are visible to a typical user. To overcome this limitation and achieve a more comprehensive coverage expression, it is necessary to consider all potential numbers of visible satellites. However, this approach significantly complicates the analysis, making it less manageable.

To address this issue, PPPs have been employed to model the spatial distribution of satellites. By utilizing a Poisson point process (PPP), the number of visible satellites becomes a random variable following a Poisson distribution. In [6], [7], the downlink coverage probability of a satellite network was derived by approximating the distribution of contact angles using the PPP-based approach. In [8], coverage and rate expressions were obtained for a noise-limited LEO satellite network. Although earlier works [3], [5]–[9] have extended the application of stochastic geometry to a finite space (a finite spherical cap), they have not achieved the same level of simplicity as in the case of an infinite 2D network plane [10]–[18]. In [4], this limitation was addressed by deriving the conditional nearest satellite distance distribution, thereby expanding the scope of satellite network analysis using stochastic geometry.

In satellite networks, the presence of buildings can obstruct propagation paths, leading to distinct propagation characteristics such as pathloss exponent, gain, and fading distribution for line-of-sight (LOS) and non-line-of-sight (NLOS) paths. Consequently, in [19], the coverage probability in shadowing channel was derived based on the PPP approach. The derived expression, however, is limited to a uniform beam gain across satellites and supported only for a signal-to-noise ratio (SNR) > 0 dB. In this regard, it is still necessary to perform a coverage analysis to find a coverage expression that is compatible with a general beam gain and supported for any SNR.

This paper provides a analysis of coverage in satellite downlink networks, considering the influence of shadowing effects. By leveraging stochastic geometry techniques, we model the satellite networks as a PPP within a finite space. In the interference-limited regime, we derive an exact coverage probability expression with a nearest satellite association rule. The derived expression incorporates the beam gain of satellites, satellite density, altitude, channel fading, pathloss exponent, and LOS probability. Simulations confirm the accuracy of the derived expression for any SNR values, offering valuable insights into satellite networks.

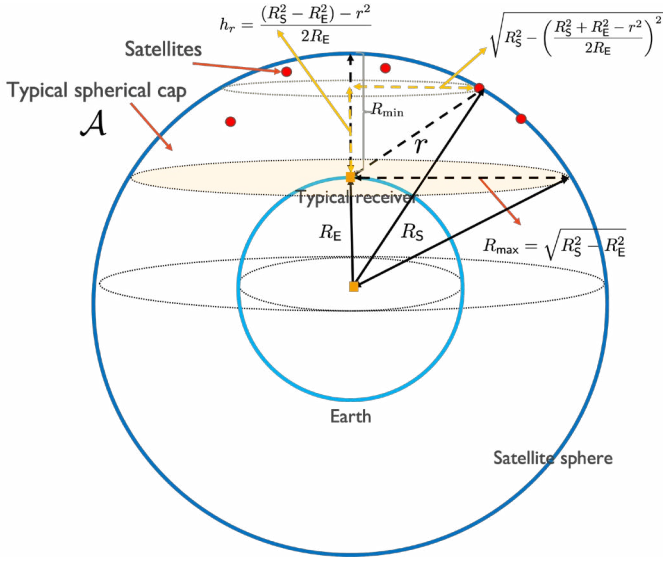

Fig. 1. In the geometry of the satellite network, the satellites are positioned on the surface of a sphere with a radius of R_{S}. A typical receiver is located at the coordinates $(0, 0, R_{\mathsf{E}})$, which represents its position above the surface of the Earth.

II. System Model

In this section, we describe the network model and the performance metrics utilized for the analysis of downlink satellite networks.

A. Preliminaries

The surface of a sphere in three-dimensional space, denoted as $\mathbb{R}^3$, is defined by having its center at the origin, represented as $\mathbf{0} \in \mathbb{R}^3$, and a fixed radius of R_{S}.

$$\mathbb{S}^2_{R_{\mathsf{S}}} = \{\mathbf{x} \in \mathbb{R}^3 : \|\mathbf{x}\|_2 = R_{\mathsf{S}}\}. \tag{1}$$

A point vector $\mathbf{x} \in \mathbb{S}^2_{R_{\mathsf{S}}}$ can be expressed using a polar coordinate system, where it is represented by a pair of elevation and azimuth angles denoted as $0 \leq \theta \leq 2\pi$ and $0 \leq \phi \leq 2\pi$, respectively.

Consider a point process denoted as $\Phi = \{\mathbf{x}_1, \ldots, \mathbf{x}_N\}$, consisting of a finite number of elements located on the surface of a sphere $\mathbb{S}^2_{R_{\mathsf{S}}}$. This point process Φ is referred to as a homogeneous spherical Poisson point process (SPPP) if the number of points on $\mathbb{S}^2_{R_{\mathsf{S}}}$, denoted as $N = \Phi(\mathbb{S}^2_{R_{\mathsf{S}}})$, follows a Poisson random variable. The mean of this Poisson random variable is given by $\lambda|\mathbb{S}^2_{R_{\mathsf{S}}}| = 4\pi R_{\mathsf{S}}^2\lambda$, where λ represents the intensity of the point process. The probability density function (PDF) of N becomes

$$\mathbb{P}(N = n) = \exp\left(-4\pi R_{\mathsf{S}}^2\lambda\right) \frac{\left(4\pi R_{\mathsf{S}}^2\lambda\right)^n}{n!}, \tag{2}$$

where $|\mathbb{S}^2_{R_{\mathsf{S}}}| = 4\pi R_{\mathsf{S}}^2$ is the surface area of the sphere. Given N, $\{\mathbf{x}_1, \ldots, \mathbf{x}_N\}$ forms a BPP, where $\mathbf{x}_i$ is independent and uniformly distributed on the surface of the sphere.

B. Network Model

We consider that the satellites are positioned on the surface of a sphere with a radius of R. These satellite locations are distributed according to a homogeneous SPPP with a density of λ. Thus, we can represent the set of satellite locations as $\Phi = \{\mathbf{x}_1, \ldots, \mathbf{x}_N\}$ where N follows a Poisson distribution with a mean of $4\lambda\pi R_{\mathsf{S}}^2$. Each satellite operates with a transmit power of P. Additionally, we have a collection of downlink users. The surface of the Earth, denoted as $\mathbb{S}^2_{R_{\mathsf{E}}}$, has a radius of R_{E}. The user locations on $\mathbb{S}^2_{R_{\mathsf{E}}}$ are assumed to follow a homogeneous SPPP with a density of λ_{U}. Thus, we can represent the set of user locations as $\Phi_{\mathsf{U}} = \{\mathbf{u}_1, \ldots, \mathbf{u}_M\}$, where M follows a Poisson distribution with a mean of $4\lambda_{\mathsf{U}}\pi R_{\mathsf{E}}^2$. It is important to note that the user point process Φ_{U} is assumed to be independent of the underlying satellite placement process Φ.

By assuming that both Φ and Φ_{U} follow homogeneous SPPPs on $\mathbb{S}^2_{R_{\mathsf{S}}}$ and $\mathbb{S}^2_{R_{\mathsf{E}}}$ respectively, the statistical distribution of Φ concerning any point in Φ_{U} remains unchanged under rotation in $\mathbb{R}^3$. This property, known as Slivnyak's theorem [10], allows us to consider a typical user located at $(0, 0, R_{\mathsf{E}})$ on $\mathbb{S}^2_{R_{\mathsf{E}}}$ without loss of generality. As shown in Fig. 1, we define a typical spherical cap denoted as $\mathcal{A}$ within the field of view of the typical receiver's location. The typical spherical cap represents the portion of the sphere $\mathbb{S}^2_{R_{\mathsf{S}}}$ that is intersected by a tangent plane to the sphere $\mathbb{S}^2_{R_{\mathsf{E}}}$ centered at $(0, 0, R_{\mathsf{E}})$. According to Archimedes' Hat-Box Theorem [20], the area of the typical spherical cap is given by

$$|\mathcal{A}| = 2\pi(R_{\mathsf{E}} - R_{\mathsf{S}})R_{\mathsf{S}}. \tag{3}$$

Additionally, we define a spherical cap that encompasses the points located within a distance of r from the typical receiver's location as follows:

$$\mathcal{A}_r = \{\mathbf{x} \in \mathbb{S}^2_{R_{\mathsf{S}}} : \|\mathbf{x} - (0, 0, R_{\mathsf{E}})\|_2 \leq r\} \subset \mathcal{A}. \tag{4}$$

To simplify the analysis, we can focus on the performance of a downlink user located within the typical spherical cap without loss of generality. Throughout this paper, we use $\mathbf{u}_1$ to indicate the typical receiver.

C. Pathloss and Channel Models

The wireless channel propagation is modeled by incorporating both path-loss attenuation and small-scale fading. The classical path-loss model, which considers the distance between satellite i and the typical user, is adopted:

$$\|\mathbf{x}_i - \mathbf{u}_1\|^{-\alpha_i} = r_i^{-\alpha_i} \tag{5}$$

where $\alpha_i \in \{\alpha^{\mathsf{LOS}}, \alpha^{\mathsf{NLOS}}\}$ when satellite i experiences LOS propagation and NLOS propagation, respectively.

Now, we incorporate the transmit and receive beam gains involved in the communication between satellites and the typical user. The effective antenna gain for the signal path from satellite i to the receiver is denoted as G_i. To simplify the analysis, we assume that the receive beam is perfectly aligned with the antenna boresight of the nearest serving satellite.

However, for interfering satellites, we assume that the receive beam is misaligned with their antenna boresights. Then, the effective antenna gain of the associated satellite and the typical receiver is $G_{\mathrm{A}} = G_{\mathrm{A}}^{\mathrm{t}} G^{\mathrm{r}} \frac{c^2}{(4\pi f_c)^2}$, and that of the interfering satellite and the typical receiver is $G_i = G_i^{\mathrm{t}} G^{\mathrm{r}} \frac{c^2}{(4\pi f_c)^2}$, where $G_{\mathrm{A}}^{\mathrm{t}}$ and G_i^{t} are the transmit antenna gains of the associated satellite and interfering satellite i, respectively, G^{r} denotes the receive antenna gain of the typical receiver, f_c denotes carrier frequency, and c is the speed of light. We note that the antenna gain model used in our analysis is based on a two-lobe approximation of the antenna radiation pattern, which has been previously discussed in works such as [21], [22].

We model the randomness of small-scale channel fading process using a distance-dependent LOS probability function $p_{\mathsf{LOS}}(r)$: the probability that a satellite located distance r away from the typical receiver experiences LOS propagation. Let H_i be the fading from satellite i to the typical receiver. Then, the distribution of the small-scale channel fading is expressed as

$$\begin{aligned} &f_{\sqrt{H_i}}(x) \\ &= p_{\mathsf{LOS}}(r_i) f_{\sqrt{H_i}|\mathsf{LOS}}(x) + (1 - p_{\mathsf{LOS}}(r_i)) f_{\sqrt{H_i}|\mathsf{NLOS}}(x). \end{aligned} \tag{6}$$

For the LOS fading channel $f_{\sqrt{H_i}|\mathsf{LOS}}(x)$, we assume the Nakagami-m distribution to suitably capture the LOS effects. Assuming $\mathbb{E}[H_i] = 1$, the probability density function (PDF) of $\sqrt{H_i}$ is given by [23]:

$$f_{\sqrt{H_i}|\mathsf{LOS}}(x) = \frac{2m^m}{\Gamma(m)} x^{2m-1} \exp\left(-mx^2\right) \tag{7}$$

for $x \geq 0$. For the NLOS fading channel $f_{\sqrt{H}|\mathsf{NLOS}}(x)$, we consider a Rayleigh distribution. Since the Nakagami-m distribution reduces to the Rayleigh distribution when $m = 1$, $f_{H|\mathsf{NLOS}}(x)$ can be directly derived from (7) by setting $m = 1$. Further, by tuning its parameter m, it is possible to model the signal fading conditions spanning from severe to moderate, while making the distribution fit to empirically measured fading data sets. For example, when $m = \frac{(K+1)^2}{2K+1}$, (7) resorts to the Rician-K distribution.

D. Performance Metric

We assume that the typical receiver is served by the associated satellite. Let $\mathbf{x}_i \in \Phi$ be the location of the associated satellite, the signal-to-interference-puls-noise (SINR) experienced by the typical receiver located at $\mathbf{u}_1 = (0, 0, R_{\mathsf{E}})$ is

$$\mathsf{SINR} = \frac{G_{\mathrm{A}} P H_i \|\mathbf{x}_i - \mathbf{u}_1\|^{-\alpha_i}}{\sum_{\mathbf{x}_j \in \Phi_{\mathrm{I}(\mathbf{x}_i)}} G_{\mathrm{I}} P H_j \|\mathbf{x}_j - \mathbf{u}_1\|^{-\alpha_j} + \sigma^2}, \tag{8}$$

where σ^2 denotes the noise power, H_i denotes fading power from satellite i to the receiver, $\Phi_{\mathrm{I}(\mathbf{x}_i)} = \Phi \cap \mathcal{A} \backslash \{\mathbf{x}_i\}$ for the strongest association, $\Phi_{\mathrm{I}(\mathbf{x}_i)} = \Phi \cap \mathcal{A}_{r_i}^c$ for the nearest association, and $\mathcal{A}_{r_i}^c = \mathcal{A} \setminus \mathcal{A}_{r_i}$ denotes the surface of the spherical cap $\mathcal{A}$ outside of $\mathcal{A}_{r_i}$.

Let $\Phi(\mathcal{A})$ represent the number of satellites in $\mathcal{A}$. Then we characterize the coverage probability for the case where there is at least one satellite exists in $\mathcal{A}$. , i.e., $\Phi(\mathcal{A}) > 0$. Accordingly, the conditional coverage probability is given as

$$\begin{aligned} &P_{\mathsf{SINR}|\Phi(\mathcal{A})>0}^{\mathsf{cov}}(\gamma; \lambda, \alpha, R_{\mathsf{S}}, m) \\ &= \mathbb{P}\left[\mathsf{SINR} \geq \gamma \mid \Phi(\mathcal{A}) > 0\right] \\ &= \mathbb{P}\left[\frac{H_i \|\mathbf{x}_i - \mathbf{u}_1\|^{-\alpha_i}}{\sum_{\mathbf{x}_j \in \Phi_{\mathrm{I}(\mathbf{x}_i)}} \bar{G}_{\mathrm{I}} H_j \|\mathbf{x}_j - \mathbf{u}_1\|^{-\alpha_j} + \bar{\sigma}^2} \geq \gamma \middle| \Phi(\mathcal{A}) > 0 \right], \end{aligned} \tag{9}$$

where $\bar{\sigma}^2 = \frac{\sigma^2}{P G_{\mathrm{A}}}$ and $\bar{G}_{\mathrm{I}} = \frac{G_{\mathrm{I}}}{G_{\mathrm{A}}} < 1$. The conditional coverage probability refers to the probability distribution of the SINR experienced by the typical receiver in the presence of any satellite base station (BS) within the spherical cap area $\mathcal{A}$. It quantifies the likelihood of achieving a certain level of SINR given the presence of at least one satellite BS in the specified region.

We further obtain the coverage probability by averaging it over all possible geometries of satellite BSs as

$$\begin{aligned} &P_{\mathsf{SINR}}^{\mathsf{cov}}(\gamma; \lambda, \alpha, R_{\mathsf{S}}, m) \\ &= P_{\mathsf{SINR}|\Phi(\mathcal{A})>0}^{\mathsf{cov}}(\gamma; \lambda, \alpha, R_{\mathsf{S}}, m) \mathbb{P}[\Phi(\mathcal{A}) > 0]. \end{aligned} \tag{10}$$

This average coverage probability provides a comprehensive assessment of the system's performance, taking into account various configurations and distributions of the satellite BSs in the spherical cap area $\mathcal{A}$.

Lemma 1 (The conditional nearest satellite distance distribution)**.** *Let $R = \min_{\mathbf{x}_i \in \Phi \cap \mathcal{A}} \|\mathbf{x}_i - \mathbf{u}_1\|_2$ be the nearest distance from the typical user's location $\mathbf{u}_1 = (0, 0, R_{\mathsf{E}})$ to a satellite in $\Phi \cap \mathcal{A}$. Then, the PDF of R is [4]*

$$f_{R|\Phi(\mathcal{A})>0}(r) = \begin{cases} \nu(\lambda, R_{\mathsf{S}}) r e^{-\lambda \pi \frac{R_{\mathsf{S}}}{R_{\mathsf{E}}} r^2} & \text{for } R_{\min} \leq r \leq R_{\max} \\ 0 & \text{otherwise,} \end{cases}$$

where $\nu(\lambda, R_{\mathsf{S}}) = 2\pi\lambda \frac{R_{\mathsf{S}}}{R_{\mathsf{E}}} \frac{e^{\lambda \pi \frac{R_{\mathsf{S}}}{R_{\mathsf{E}}} \left(R_{\mathsf{S}}^2 - R_{\mathsf{E}}^2\right)}}{e^{2\lambda\pi R_{\mathsf{S}}(R_{\mathsf{S}} - R_{\mathsf{E}})} - 1}$, $R_{\min} = R_{\mathsf{S}} - R_{\mathsf{E}}$, and $R_{\max} = \sqrt{R_{\mathsf{S}}^2 - R_{\mathsf{E}}^2}$.

Proof. See the proof of Lemma 2 in [4]. ■

Lemma 2. *Conditioned on that the distance between the typical receiver and the associated satellite is r and $\Phi(\mathcal{A}) > 0$, the Laplace transform of the aggregated interference power for the nearest satellite association policy is derived as* (11) *on the top of the next page.*

Proof. Let $\mathbf{x}_i$ be the associated satellite. Then we define the aggregated interference power conditioned on $\Phi(\mathcal{A}) > 0$ and $\|\mathbf{x}_i - \mathbf{u}_1\| = r_i$ for both the strongest and the nearest satellite association policies as

$$I_{r_i} = \sum_{\mathbf{x}_j \in \Phi_{\mathrm{I}(\mathbf{x}_i)}} \bar{G}_{\mathrm{I}} H_j \|\mathbf{x}_j - \mathbf{u}_1\|^{-\alpha_j}, \tag{12}$$

where $\Phi_{\mathrm{I}(\mathbf{x}_i)} = \Phi \backslash \{\mathbf{x}_i\}$ for the strongest association, $\Phi_{\mathrm{I}(\mathbf{x}_i)} = \Phi \cap \mathcal{A}_{r_i}^c$ for the nearest association, and $\mathcal{A}_{r_i}^c = \mathcal{A} \backslash \mathcal{A}_{r_i}$ denotes the set of satellites on the spherical cap outside $\mathcal{A}_{r_i}$. Without loss of generality, we assume $\mathbf{x}_i = \mathbf{x}_1$ and $r_i = r$.

$$\mathcal{L}_{I_r|\Phi(\mathcal{A})>0,r}(s)=\exp\left(-2\pi\lambda\frac{R_{\mathsf{S}}}{R_{\mathsf{E}}}\int_r^{R_{\max}}\left(1-p_{\mathsf{LOS}}(v)\frac{1}{\left(1+\frac{s\bar{G}_{\mathrm{I}}v^{-\alpha^{\mathsf{LOS}}}}{m}\right)^m}-p_{\mathsf{NLOS}}\frac{1}{1+s\bar{G}_{\mathrm{I}}v^{-\alpha^{\mathsf{NLOS}}}}\right)v\ \mathrm{d}v\right) \tag{11}$$

Since H_j is the Nakagami-m random variable for the LOS channel fading, the complementary cumulative distribution function (CCDF) of H_j for LOS channels is

$$\mathbb{P}[H_j^{\mathsf{LOS}}\geq x]=e^{-mx}\sum_{k=0}^{m-1}\frac{(mx)^k}{k!}. \tag{13}$$

The CCDF of H_j for NLOS channels which follow Rayleigh fading distribution is given as

$$\mathbb{P}[H_j^{\mathsf{NLOS}}\geq x]=e^{-x}. \tag{14}$$

We compute the Laplace transform of the aggregated interference power as

$$\begin{aligned}
&\mathcal{L}_{I_r|\Phi(\mathcal{A})>0,r}(s) && (15)\\
&=\mathbb{E}\left[e^{-sI_r}\ \middle|\ r,\Phi(\mathcal{A})>0\right] && (16)\\
&=\mathbb{E}\left[\prod_{\mathbf{x}_j\in\Phi_{\mathrm{I}(\mathbf{x}_1)}}e^{-s\bar{G}_{\mathrm{I}}H_jr_j^{-\alpha_j}}\ \middle|\ r,\Phi(\mathcal{A})>0\right] && (17)\\
&\overset{(a)}{=}\mathbb{E}_{\Phi}\Bigg[\prod_{\mathbf{x}_j\in\Phi_{\mathrm{I}(\mathbf{x}_1)}}\Big(p_{\mathsf{LOS}}(r_j)\mathbb{E}_{H_j^{\mathsf{LOS}}}\left[e^{-s\bar{G}_{\mathrm{I}}H_j^{\mathsf{LOS}}r_j^{-\alpha^{\mathsf{LOS}}}}\right] && (18)\\
&+p_{\mathsf{NLOS}}(r_j)\mathbb{E}_{H_j^{\mathsf{NLOS}}}\left[e^{-s\bar{G}_{\mathrm{I}}H_j^{\mathsf{NLOS}}r_j^{-\alpha^{\mathsf{NLOS}}}}\right]\Big)\ \Bigg|\ r,\Phi(\mathcal{A})>0\Bigg]
\end{aligned}$$

where (a) comes from the PDFs of LOS and NLOS probability distributions in (6). Regarding the nearest association, they can reside only in $\mathcal{A}_r^c$. Accordingly, let $\mathcal{A}_{\mathrm{I}}\in\{\mathcal{A},\mathcal{A}_r^c\}$ which is determined by the association policy. Then from the probability generating functional (PGFL) of the PPP [11], [14], (18) further becomes

$$\begin{aligned}
&\exp\Bigg(-\lambda\int_{\mathbf{x}_i\in\mathcal{A}_{\mathrm{I}}}\Big(1-p_{\mathsf{LOS}}(r_i)\mathbb{E}_{H_i^{\mathsf{LOS}}}\left[e^{-s\bar{G}_{\mathrm{I}}H_i^{\mathsf{LOS}}r_i^{-\alpha^{\mathsf{LOS}}}}\right]\\
&\quad-p_{\mathsf{NLOS}}(r_i)\mathbb{E}_{H_i^{\mathsf{NLOS}}}\left[e^{-s\bar{G}_{\mathrm{I}}H_i^{\mathsf{NLOS}}r_i^{-\alpha^{\mathsf{NLOS}}}}\right]\Big)\ \mathrm{d}\mathbf{x}_i\Bigg)\\
&=\exp\Bigg(-\lambda\int_{\mathbf{x}_i\in\mathcal{A}_{\mathrm{I}}}\Bigg(1-p_{\mathsf{LOS}}(r_i)\frac{1}{\left(1+\frac{s\bar{G}_{\mathrm{I}}r_i^{-\alpha^{\mathsf{LOS}}}}{m}\right)^m}\\
&\quad-p_{\mathsf{NLOS}}(r_i)\frac{1}{1+s\bar{G}_{\mathrm{I}}r_i^{-\alpha^{\mathsf{NLOS}}}}\Bigg)\ \mathrm{d}\mathbf{x}_i\Bigg)\\
&\overset{(b)}{=}\exp\Bigg(-2\pi\lambda\frac{R_{\mathsf{S}}}{R_{\mathsf{E}}}\int_r^{R_{\max}}\Bigg(1-p_{\mathsf{LOS}}(v)\frac{1}{\left(1+\frac{s\bar{G}_{\mathrm{I}}v^{-\alpha^{\mathsf{LOS}}}}{m}\right)^m}\\
&\quad-p_{\mathsf{NLOS}}(v)\frac{1}{1+s\bar{G}_{\mathrm{I}}v^{-\alpha^{\mathsf{NLOS}}}}\Bigg)\ v\mathrm{d}v\Bigg) \qquad (19)
\end{aligned}$$

where (b) comes from $\frac{\partial|\mathcal{A}_v|}{\partial v}=2\pi\frac{R_{\mathsf{S}}}{R_{\mathsf{E}}}v$. This completes the proof. ■

Theorem 1. *In the interference-limited regime, i.e., $\bar{\sigma}^2\to 0$, the coverage probability of the typical receiver for the nearest satellite association policy is* (20) *on the top of the next page, where $\bar{\nu}_{\mathsf{n}}(\lambda,R_{\mathsf{s}})=\nu(\lambda,R_{\mathsf{s}})\left(1-e^{-\lambda 2\pi(R_{\mathsf{S}}-R_{\mathsf{E}})R_{\mathsf{S}}}\right)$.*

Proof. Without loss of generality, we assume $\mathbf{x}_i=\mathbf{x}_1$ and $r_i=r$ in this proof. For the nearest satellite association, we first compute the coverage probability conditioned on $\|\mathbf{x}_1-\mathbf{u}_1\|=r$ and $\Phi(\mathcal{A})>0$ with $\bar{\sigma}^2\to 0$ as

$$\begin{aligned}
&P^{\mathsf{cov}}_{\mathsf{SIR}|\Phi(\mathcal{A})>0}(\gamma;\lambda,\alpha,R_{\mathsf{S}},m)\\
&=\mathbb{E}_r\Big[\mathbb{P}\big(H_1\geq r^{\alpha}\gamma I_r\mid r\big)\Big|\Phi(\mathcal{A})>0\Big] && (21)\\
&\overset{(a)}{=}\mathbb{E}_r\Bigg[\mathbb{E}_{I_r}\Big[p_{\mathsf{LOS}}(r)\mathbb{P}\big(H_1^{\mathsf{LOS}}\geq r^{\alpha^{\mathsf{LOS}}}\gamma I_r\mid I_r\big)\\
&\qquad+p_{\mathsf{NLOS}}(r)\mathbb{P}\big(H_1^{\mathsf{NLOS}}\geq r^{\alpha^{\mathsf{NLOS}}}\gamma I_r\mid I_r\big)\Big|r\Big]\Bigg|\Phi(\mathcal{A})>0\Bigg]\\
&=\mathbb{E}_r\Bigg[p_{\mathsf{LOS}}(r)\mathbb{E}_{I_r}\left[\sum_{k=0}^{m-1}\frac{m^k\gamma^kr^{k\alpha^{\mathsf{LOS}}}}{k!}I_r^ke^{-mr^{\alpha^{\mathsf{LOS}}}\gamma I_r}\middle|r\right]\\
&\quad+p_{\mathsf{NLOS}}(r)\mathbb{E}_{I_r}\left[e^{-r^{\alpha^{\mathsf{NLOS}}}\gamma I_r}\middle|r\right]\Bigg|\Phi(\mathcal{A})>0\Bigg] && (22)
\end{aligned}$$

where (a) follows from the PDF of LOS/NLOS distribution in (6). Then by using Lemma 2 and applying the derivative property of the Laplace transform, i.e., $\mathbb{E}\left[X^ke^{-sX}\right]=(-1)^k\frac{\mathrm{d}^k\mathcal{L}_X(s)}{\mathrm{d}s^k}$, (22) further becomes

$$\begin{aligned}
&\mathbb{E}_r\Bigg[p_{\mathsf{LOS}}(r)\sum_{k=0}^{m-1}\frac{(-m\gamma r^{\alpha^{\mathsf{LOS}}})^k}{k!}\cdot\frac{\mathrm{d}^k\mathcal{L}_{I_{r|\Phi(\mathcal{A})>0,r}}(s)}{\mathrm{d}s^k}\Bigg|_{s=m\gamma r^{\alpha^{\mathsf{LOS}}}}\\
&\quad+p_{\mathsf{NLOS}}(r)\ \mathcal{L}_{I_{r|\Phi(\mathcal{A})>0,r}}(z)\big|_{z=\gamma r^{\alpha^{\mathsf{NLOS}}}}\Bigg|\Phi(\mathcal{A})>0\Bigg] && (23)\\
&\overset{(b)}{=}\nu(\lambda,R_{\mathsf{S}})\times\\
&\int_{R_{\min}}^{R_{\max}}\Bigg(p_{\mathsf{LOS}}(r)\sum_{k=0}^{m-1}\frac{(-m\gamma r^{\alpha^{\mathsf{LOS}}})^k}{k!}\cdot\frac{\mathrm{d}^k\mathcal{L}_{I_{r|\Phi(\mathcal{A})>0,r}}(s)}{\mathrm{d}s^k}\Bigg|_{s=m\gamma r^{\alpha^{\mathsf{LOS}}}}\\
&\quad+p_{\mathsf{NLOS}}(r)\ \mathcal{L}_{I_{r|\Phi(\mathcal{A})>0,r}}(z)\big|_{z=\gamma r^{\alpha^{\mathsf{NLOS}}}}\Bigg)re^{-\lambda\pi\frac{R_{\mathsf{S}}}{R_{\mathsf{E}}}r^2}\mathrm{d}r && (24)
\end{aligned}$$

where (b) is from the expectation over the nearest satellite distribution derived in Lemma 1. Multiplying $\mathbb{P}[\Phi(\mathcal{A})>0]=1-e^{-\lambda 2\pi(R_{\mathsf{S}}-R_{\mathsf{E}})R_{\mathsf{S}}}$ to (24) completes the proof. ■

$$P_{\mathsf{SIR}}^{\mathsf{cov}}(\gamma;\lambda,\alpha,R_{\mathsf{S}},m)=\bar{\nu}_{\mathsf{n}}(\lambda,R_{\mathsf{S}})\times \tag{20}$$
$$\int_{R_{\min}}^{R_{\max}}\left(p_{\mathsf{LOS}}(r)\sum_{k=0}^{m-1}\frac{m^k\gamma^k r^{k\alpha^{\mathsf{LOS}}}}{k!}(-1)^k\frac{\mathrm{d}^k\mathcal{L}_{I_{r|\Phi(\mathcal{A})>0,r}}(s)}{\mathrm{d}s^k}\bigg|_{s=m\gamma r^{\alpha^{\mathsf{LOS}}}}+p_{\mathsf{NLOS}}(r)\mathcal{L}_{I_{r|\Phi(\mathcal{A})>0,r}}(z)\big|_{z=\gamma r^{\alpha^{\mathsf{NLOS}}}}\right)re^{-\lambda\pi\frac{R_{\mathsf{S}}}{R_{\mathsf{E}}}r^2}\mathrm{d}r$$

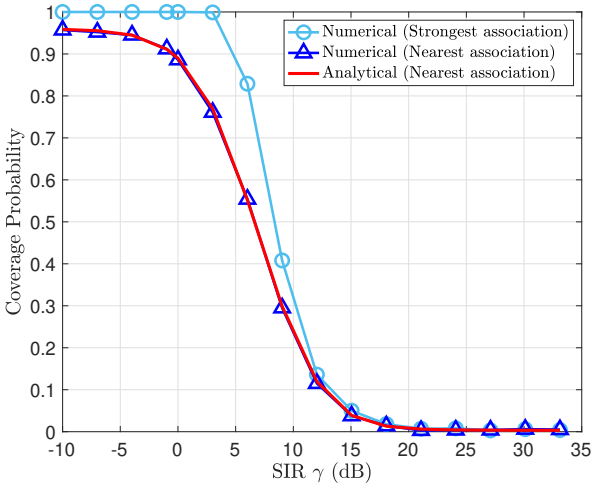

Fig. 2. The coverage probability from numerical and theoretical results for $K=10,\beta=0.048,\alpha_{\mathsf{LOS}}=2,\alpha_{\mathsf{NLOS}}=3,m=2$, and $h=500$ km.

III. Simulation Results

In simulations, we first validate the accuracy of the derived coverage expression by comparing it with the results obtained from the simulation. This step allows us to ensure that the analytical model aligns with the empirical observations. We set $h=500$ km which is 500 km. Additionally, we consider $m=2$ as a specific value for our analysis. Regarding the beam gain, we set $\bar{G}_{\mathrm{I}}=-10$ dB. For the purpose of simulations, we define the average number of satellites within the typical spherical cap as K, where K is given by $K=\lambda|\mathcal{A}|$. For the distance-dependent LOS and NLOS propagation probability, we adopt the following exponential blockage probability distribution [24]:

$$p_{\mathsf{LOS}}(r)=\exp\left(-\beta\cot\left(\arcsin\left(\frac{R_{\mathsf{S}}^2-R_{\mathsf{E}}^2}{2rR_{\mathsf{E}}}-\frac{r}{2R_{\mathsf{E}}}\right)\right)\right),$$

where $\beta\geq 0$ is related to the geometry of the urban environment and plays a crucial role in our analytic model. It determines the LOS probability, which represents the likelihood of having a clear line of sight between the transmitter and receiver in a given urban scenario. This model has been validated against collected LOS probabilities from the 3GPP model [24], [25], demonstrating reasonable agreement between the two. We adopt a specific value of $\beta=0.048$, which is suitable for the sub-urban scenario.

Fig. 2 shows the coverage probabilties for the considered system obtained from a numerical result and the derived theoretical expression under the nearest association rule. The numerical coverage result with the strongest association rule. We observe that the theoretical coverage probability exactly matches with the numerical one, which validate the expression. In addition, the coverage probability with the nearest association rule performs as a lower bound of the one with the strongest association rule. Therefore, it is concluded that the derived coverage expression can be considered as a lower bound of the satellite network coverage with incorporating the beam gain, and available for any SNR regime.

IV. Conclusion

This paper investigates the coverage performance of satellite networks in the presence of shadowing by employing stochastic geometry tools. By considering channel propagation conditions and utilizing a distance-dependent LOS probability function, we derive an analytical expression for the coverage probability with the nearest satellite association rule. The derived coverage probability exactly aligned with a numerical coverage probability, which validates the derived theorem. In addition, it is concluded that the derived coverage expression can be considered as a lower bound of the satellite network coverage with incorporating the beam gain, and available for any SNR regime. Consequently, the derived coverage probability offers valuable insights for satellite deployment policies, taking into account the effect of channel shadowing. These findings contribute to a better understanding of satellite network performance and aid in making informed decisions regarding system design and optimization.

Acknowledgement

This work was supported by Korea Research Institute for defense Technology planning and advancement (KRIT) - grant funded by the Defense Acquisition Program Administration (DAPA) (KRIT-CT-22-040).

References

[1] S. Liu, Z. Gao, Y. Wu, D. W. K. Ng, X. Gao, K.-K. Wong, S. Chatzinotas, and B. Ottersten, "LEO satellite constellations for 5G and beyond: How will they reshape vertical domains?" *IEEE Commun. Mag.*, vol. 59, no. 7, pp. 30–36, 2021.

[2] M. Giordani and M. Zorzi, "Non-terrestrial networks in the 6G era: Challenges and opportunities," *IEEE Network*, vol. 35, no. 2, pp. 244–251, 2020.

[3] N. Okati, T. Riihonen, D. Korpi, I. Angervuori, and R. Wichman, "Downlink coverage and rate analysis of low Earth orbit satellite constellations using stochastic geometry," *IEEE Trans. on Commun.*, vol. 68, no. 8, pp. 5120–5134, 2020.

[4] J. Park, J. Choi, and N. Lee, "A Tractable Approach to Coverage Analysis in Downlink Satellite Networks," *IEEE Trans. Wireless Commun.*, 2022.

[5] A. Talgat, M. A. Kishk, and M.-S. Alouini, "Stochastic geometry-based analysis of LEO satellite communication systems," *IEEE Commun. Lett.*, vol. 25, no. 8, pp. 2458–2462, 2020.

[6] A. Al-Hourani, "An analytic approach for modeling the coverage performance of dense satellite networks," *IEEE Wireless Commun. Lett.*, vol. 10, no. 4, pp. 897–901, 2021.
[7] ——, "Optimal satellite constellation altitude for maximal coverage," *IEEE Wireless Commun. Lett.*, vol. 10, no. 7, pp. 1444–1448, 2021.
[8] N. Okati and T. Riihonen, "Modeling and analysis of LEO mega-constellations as nonhomogeneous Poisson point processes," in *IEEE Veh. Technol. Conf.*, 2021, pp. 1–5.
[9] A. Talgat, M. A. Kishk, and M.-S. Alouini, "Nearest neighbor and contact distance distribution for binomial point process on spherical surfaces," *IEEE Commun. Lett.*, vol. 24, no. 12, pp. 2659–2663, 2020.
[10] F. Baccelli and B. Błaszczyszyn, "Stochastic geometry and wireless networks: Volume I," *Foundations and Trends® in Networking*, vol. 3, no. 3–4, pp. 249–449, 2009.
[11] F. Baccelli, B. Blaszczyszyn, and P. Muhlethaler, "An Aloha protocol for multihop mobile wireless networks," *IEEE Trans. Inform. Theory*, vol. 52, no. 2, pp. 421–436, 2006.
[12] M. Haenggi, "A geometric interpretation of fading in wireless networks: Theory and applications," *IEEE Trans. Inform. Theory*, vol. 54, no. 12, pp. 5500–5510, 2008.
[13] F. Baccelli, B. Blaszczyszyn, and P. Muhlethaler, "Stochastic analysis of spatial and opportunistic Aloha," *IEEE J. Sel. Areas Commun.*, vol. 27, no. 7, pp. 1105–1119, 2009.
[14] M. Haenggi, J. G. Andrews, F. Baccelli, O. Dousse, and M. Franceschetti, "Stochastic geometry and random graphs for the analysis and design of wireless networks," *IEEE J. Sel. Areas Commun.*, vol. 27, no. 7, pp. 1029–1046, 2009.
[15] J. G. Andrews, F. Baccelli, and R. K. Ganti, "A tractable approach to coverage and rate in cellular networks," *IEEE Trans. Commun.*, vol. 59, no. 11, pp. 3122–3134, 2011.
[16] H. S. Dhillon, R. K. Ganti, F. Baccelli, and J. G. Andrews, "Modeling and analysis of K-tier downlink heterogeneous cellular networks," *IEEE J. Sel. Areas Commun.*, vol. 30, no. 3, pp. 550–560, 2012.
[17] M. Di Renzo, A. Guidotti, and G. E. Corazza, "Average rate of downlink heterogeneous cellular networks over generalized fading channels: A stochastic geometry approach," *IEEE Trans. Commun.*, vol. 61, no. 7, pp. 3050–3071, 2013.
[18] N. Lee, X. Lin, J. G. Andrews, and R. W. Heath, "Power control for D2D underlaid cellular networks: Modeling, algorithms, and analysis," *IEEE J. Sel. Areas Commun.*, vol. 33, no. 1, pp. 1–13, 2014.
[19] J. Choi, J. Park, J. Lee, , and N. Lee, "Coverage Analysis for Downlink Satellite Networks: Effect of Shadowing," in *IEEE Int. Conf. Commun.*, 2023, to appear.
[20] H. Cundy and A. Rollett, "Sphere and cylinder–archimedes' Theorem," *Mathematical Models, 3rd ed.,* Stradbroke, England: Tarquin Pub., pp. 172–173, 1989.
[21] M. Di Renzo, "Stochastic geometry modeling and analysis of multi-tier millimeter wave cellular networks," *IEEE Trans. Wireless Commun.*, vol. 14, no. 9, pp. 5038–5057, 2015.
[22] T. Bai, A. Alkhateeb, and R. W. Heath, "Coverage and capacity of millimeter-wave cellular networks," *IEEE Commun. Mag.*, vol. 52, no. 9, pp. 70–77, 2014.
[23] G. Giunta, C. Hao, and D. Orlando, "Estimation of Rician K-factor in the presence of Nakagami-m shadowing for the LoS component," *IEEE Wireless Commun. Lett.*, vol. 7, no. 4, pp. 550–553, 2018.
[24] A. Al-Hourani and I. Guvenc, "On modeling satellite-to-ground path-loss in urban environments," *IEEE Commun. Lett.*, vol. 25, no. 3, pp. 696–700, 2020.
[25] 3rd Generation Partnership Project, "Study on New Radio (NR) to support non-terrestrial networks (Release 15)," 2018.